Title	Electronic transitions of cobalt monoboride
Author(s)	Ng, YW; Pang, HF; Cheung, ASC
Citation	Journal of Chemical Physics, 2011, v. 135 n. 20, article no. 204308
Issued Date	2011
URL	http://hdl.handle.net/10722/148664
Rights	Copyright 2011 American Institute of Physics. This article may be downloaded for personal use only. Any other use requires prior permission of the author and the American Institute of Physics. The following article appeared in Journal of Chemical Physics, 2011, v. 135 n. 20, article no. 204308 and may be found at http://jcp.aip.org/resource/1/jcpsa6/v135/i20/p204308_s1

AIP | The Journal of Chemical Physics

Electronic transitions of cobalt monoboride

Y. W. Ng, H. F. Pang, and A. S.-C. Cheung

Citation: J. Chem. Phys. **135**, 204308 (2011); doi: 10.1063/1.3663619
View online: http://dx.doi.org/10.1063/1.3663619
View Table of Contents: http://jcp.aip.org/resource/1/JCPSA6/v135/i20
Published by the American Institute of Physics.

Electronic transitions of cobalt monoboride

Y. W. Ng, H. F. Pang, and A. S.-C. Cheung[a)]
Department of Chemistry, The University of Hong Kong, Pokfulam Road, Hong Kong

(Received 21 August 2011; accepted 2 November 2011; published online 30 November 2011)

Electronic transition spectrum of cobalt monoboride (CoB) in the visible region between 495 and 560 nm has been observed and analyzed using laser-induced fluorescence spectroscopy. CoB molecule was produced by the reaction of laser-ablated cobalt atom and diborane (B_2H_6) seeded in argon. Fifteen vibrational bands with resolved rotational structure have been recorded, which included transitions of both $Co^{10}B$ and $Co^{11}B$ isotopic species. Our analysis showed that the observed transition bands are $\Delta\Omega = 0$ transitions with $\Omega'' = 2$ and $\Omega'' = 3$ lower states. Four transition systems have been assigned, namely, the $[18.1]^3\Pi_2$–$X^3\Delta_2$, the $[18.3]^3\Phi_3$–$X^3\Delta_3$, the [18.6]3– $X^3\Delta_3$, and the [19.0]2–$X^3\Delta_2$ systems. The bond length, r_o, of the $X^3\Delta_3$ state of CoB is determined to be 1.705 Å. The observed rotational lines showed unresolved hyperfine structure arising from the nuclei, which conforms to the Hund's case (a_β) coupling scheme. This work represents the first experimental investigation of the CoB spectrum. © *2011 American Institute of Physics*. [doi:10.1063/1.3663619]

I. INTRODUCTION

Many transition metal (TM) borides are known catalysts for the hydrogenation of alkenes and alkynes, reduction of nitrogenous functional groups and deoxygenation reactions.[1] Besides, metal borides are also refractory compounds process remarkable physical properties such as very high conductivity (TiB_2) (Ref. 2) and even superconductivity (MgB_2),[3] and super hardness (ReB_2).[4] Recently, boron nitride nanotubes could be synthesized from zirconium boride (ZrB_2) rod in a nitrogen atmosphere using electric arc discharge.[5] Despite the chemical and physical importance, very little is known about the chemical bonding of this class of boride compounds. Since diatomic TM boride is the simplest building block of the more complicated TM boride compounds, detail knowledge of the characteristic of chemical bonding and electronic structure of this simple system would be useful for understanding large molecules and even their bulk properties.

TM borides are often used as catalysts, recently cobalt boride solid and CoB thin-film received special attention because of their ability to catalyze the production of hydrogen in the hydrolysis of sodium borohydride solution.[6,7] Sodium borohydride shows superior qualities for providing a safe and practical way for hydrogen production, the use of CoB catalyst allows good control of the hydrogen production rate. As far as the study of TM monoboride molecules is concerned, Tzeli and Mavridis[8] performed theoretical calculations on the *3d* TM monoborides aiming at understanding their chemical bonding characteristics and also their ground state symmetry. CoB was predicted to have a $X^3\Delta_i$ ground state and an equilibrium bond length, $r_e = 1.700$ Å. Among all *3d* TM monoborides only NiB (Ref. 9) has been studied experimentally, this work represents the first experimental work on the CoB molecule.

In this paper, we report the analysis of electronic transitions of the CoB molecule recorded using the technique of laser vaporization/reaction free jet expansion and laser-induced fluorescence (LIF) spectroscopy in the visible region. Spectra of both $Co^{10}B$ and $Co^{11}B$ isotopes were resolved and recorded. One of the aims in this work is to identify and characterize the ground state of CoB. Electronic configurations giving rise to the observed electronic states have also been examined using a molecular orbital energy level diagram.

II. EXPERIMENTAL

The apparatus used in the present study has been described in earlier papers.[10,11] Only a brief description of the relevant experimental conditions for obtaining the CoB spectrum is given here. Frequency-doubled Nd:YAG laser pulses with 5–6 mJ, were focused onto the surface of a cobalt rod to generate cobalt atoms. A pulsed valve with appropriate delay time released a gas mixture of 0.5% diborane (B_2H_6) in argon to react with cobalt atom to produce CoB. The Nd:YAG-pulsed valve system was operated at 10 Hz. A pulsed dye laser operated with Coumarin dyes was pumped by another Nd:YAG laser with wavelength set to 355 nm producing tunable output in the visible region, which was used to excite the jet cooled CoB molecule. The power output from the tunable dye laser was typically about 4–5 mJ, its wavelength was measured by a wavelength meter with accuracy around ± 0.02 cm^{-1}, and the laser linewidth was about 0.07 cm^{-1}. The LIF signal was directed into a monochromator and subsequently detected by a photomultiplier tube (PMT). The monochromator was used for two purposes: (i) scanned to record wavelength resolved fluorescence spectrum and (ii) acted as an optical filter in recording the LIF spectrum. The PMT output was fed into a fast oscilloscope for averaging and storage. Typical molecular transition linewidth obtained for CoB in this work was larger than 0.2 cm^{-1}, which is generally wider than the expected Doppler width. The larger width

a)Author to whom correspondence should be addressed. Electronic mail: hrsccsc@hku.hk. Tel.: (852) 2859 2155. Fax: (852) 2857 1586.

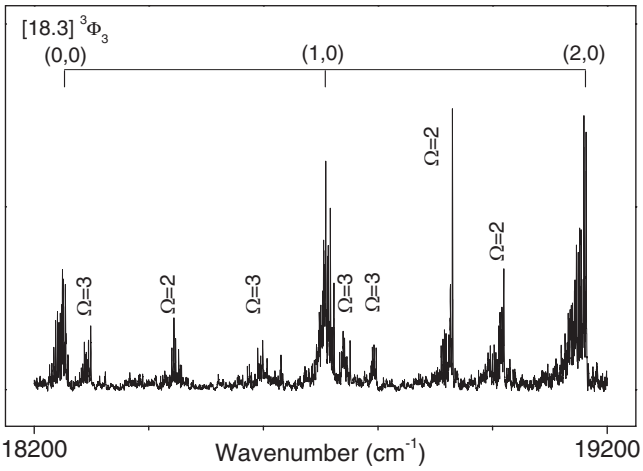

FIG. 1. Low-resolution LIF spectrum of CoB.

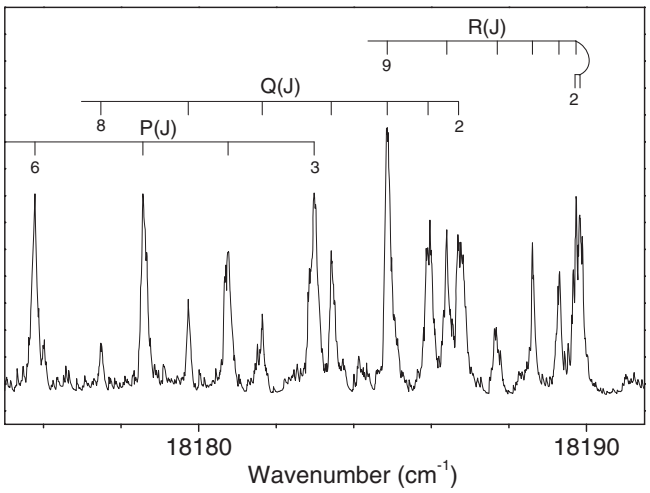

FIG. 2. The (0, 0) band of the $[18.1]^3\Pi_2$–$X^3\Delta_2$ transition of CoB.

is probably due to unresolved hyperfine structure from the Co and B nuclei.

III. RESULTS AND DISCUSSION

A. Low-resolution broadband spectrum

Low-resolution LIF spectrum of CoB in the visible region between 495 and 560 cm^{-1} has been recorded. Figure 1 is a broadband low-resolution scan of the CoB spectrum, the bands identified are $\Delta\Omega = 0$ transitions with either $\Omega'' = 2$ or $\Omega'' = 3$ value. Spectra of both isotopes $Co^{10}B$ and $Co^{11}B$ have been observed. Fifteen vibrational bands were recorded and analyzed; their upper and lower state Ω values were characterized, and their band origin and rotational constant B were obtained by least-squares fitting of the measured line positions. Further analysis was proven to be difficult, the usual regularities among vibrational bands are lacking and the grouping of these bands under an electronic transition system was not trivial. This situation is probably due to the fact that the electronic states are generally in case (c) coupling scheme and, therefore, electronic transition bands could only be characterized by individual Ω value.[12] In addition, rotational transition lines are generally broadened by unresolved hyperfine structure from both the Co and B nuclei, and thus the measurement of line positions would be of lower accuracy. In the least-squares fit, the larger uncertainty in the measurement of line positions would eventually propagate to molecular parameters such as band origin and rotational constants. Furthermore, it is generally expected that the observation of isotopic molecules could readily help the assignment of vibrational quantum number, however, for $Co^{10}B$ and $Co^{11}B$ isotopes, the isotopic shift between them is relatively large and their transition bands are crowded, which made the association of isotopic transition bands difficult. Combining problems in case (c) coupling, larger uncertainties in rotational constants and also very minimum help from isotopic shifts, among the bands measured, we managed to identify four electronic transition systems, namely, the $[18.1]^3\Pi_2$–$X^3\Delta_2$, the $[18.3]^3\Phi_3$–$X^3\Delta_3$, the [18.6]3 –$X^3\Delta_3$, and the [19.0]2–$X^3\Delta_2$ systems.

B. $[18.1]^3\Pi_2$–$X^3\Delta_2$ transition

The (0, 0) and (0, 1) bands of this system were recorded and analyzed. Each band shows resolved P, Q, and R branches. Line assignment was straightforward. The band head region of the (0, 0) band of this transition is shown in Figure 2. The observation of the P(3), Q(2), and R(2) first lines from their corresponding branches established the vibrational band is a $\Omega' = 2$ and $\Omega'' = 2$ transition. The P and Q branches are stronger in intensity than the R branch, which is consistent with a transition with $\Delta\Lambda = -1$. Both the (0, 0) and (1, 0) bands are weak in intensity. It can be noticed easily in Figure 2 that there are unresolved structures in the low J lines and also the linewidth is wider than expected from the Doppler broadening, this is due to the hyperfine structure arising from the Co and B nuclei. The observed line positions of the vibrational bands were fit to the following expression:[12]

$$\nu = \nu_o + B'J'(J'+1) - D'[J'(J'+1)]^2 - \{B''J''(J''+1) - D''[J''(J''+1)]^2\}, \quad (1)$$

where the $'$ and $''$ refer to the upper and lower states, respectively. The ν_o is the band origin, and B and D are rotational and centrifugal distortion constants, respectively. It is because only low J lines ($J < 12$) were measured, in our least-squares fit; the D constant for both the upper and lower states was set to zero. The least-squares fit of the transition lines in these bands were performed in two stages, first band by band and, subsequently, all bands were merged together in a single fit. Determined molecular constants for individual bands are given in Table I. The assignment of the upper and lower states will be discussed in Sec. III E. A list of the measured transition line positions of the observed $[18.1]^3\Pi_2$–$X^3\Delta_2$ system is available from the supplemental material.[13] The $\Delta G_{1/2}$ measured for the $X^3\Delta_2$ is 734.68 cm^{-1}.

C. $[18.3]^3\Phi_3$–$X^3\Delta_3$ transition

As far as the intensity of vibrational bands is concerned, molecular transitions with $\Delta\Omega = 0$ and $\Omega'' = 3$ are generally stronger than those with $\Omega'' = 2$. We recorded the (3, 0),

TABLE I. Molecular constants for observed transition bands of $Co^{11}B$ (cm^{-1}).[a]

Upper state	Lower state	v′ − v″	ν_o	B′	B″	Remark
$[18.1]^3\Pi_2$	$X^3\Delta_2$	0 − 0	18 187.57	0.4914	0.6306	
		0 − 1	17 452.89	0.4914	0.6239	$\Delta G_{1/2} = 734.68$
[19.0]2	$X^3\Delta_2$	0 − 0	19 017.12	0.4896	0.6305	
		0 − 0	19 027.50	0.5308 (0.5307)[b]	0.6794 (0.6802)	$Co^{10}B$
$[18.3]^3\Phi_3$	$X^3\Delta_3$	0 − 0	18 251.99	0.4909	0.6254[c]	
		1 − 0	18 714.80	0.4818		
		2 − 0	19 160.88	0.4782		
		3 − 0	19585.42	0.4577		
		2 − 1	18 429.22	0.4783	0.6213	$\Delta G_{1/2} = 731.66$
[18.6]3	$X^3\Delta_3$	0 − 0	18 596.40	0.4874	0.6255	
		0 − 0	18 603.61	0.5344 (0.5310)	0.6757 (0.6778)	$Co^{10}B$

[a]Error limits of the band origin and the B values are ±0.03 cm^{-1} and ±0.0003 cm^{-1}, respectively.
[b]Value given in parenthesis is calculated from isotopic relationships (see text).
[c]Value obtained from a merged least-squares fit with common v = 0 level.

(2, 0), (1, 0), (0, 0) and the (2, 1) bands of this transition. Figure 3 shows the band head region of the (2, 0) band. The corresponding first lines of the P, Q, and R branches are P(4), Q(3), and R(3) lines, respectively, which confirms the band is a $\Omega' = 3$ and $\Omega'' = 3$ transition. The R and Q branches are stronger, which is consistent with a $\Delta\Lambda = +1$ transition. It is easily notice that the linewidth of the low J rotational line is wide and it is narrowing down as J increases. For instance, the Q(3) line has a linewidth of about 0.42 cm^{-1} and the Q(8) line decreases to 0.19 cm^{-1}. Such a change in linewidth behavior as a function of increasing J value is consistent with the Hund's coupling case (a_β) scheme in the hyperfine structure. The least-squares fit of the transition lines in these bands were again performed in two stages using the expression in Eq. (1). Determined molecular constants are also listed in Table I. The line list of the $[18.3]^3\Phi_3$–$X^3\Delta_3$ system transition is available from the supplemental material.[13] The vibrational separations, $\Delta G_{1/2}$, $\Delta G_{3/2}$, and $\Delta G_{5/2}$ of the $[18.3]^3\Phi_3$ state are, respectively, 462.81, 446.08, and 424.56 cm^{-1}, and the equilibrium molecular constants determined are $T_e = 18012.6$, $\omega_e = 482.9$, and $\omega_e\chi_e = 9.5$ cm^{-1}. The $\Delta G_{1/2}$ for the $X^3\Delta_3$ was measured to be 731.66 cm^{-1}.

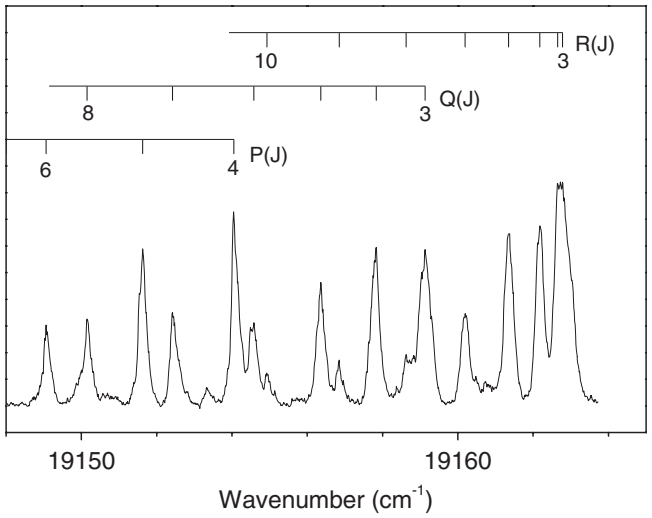

FIG. 3. The (2, 0) band of the $[18.3]^3\Phi_3$–$X^3\Delta_3$ transition of CoB.

D. [18.6]3–$X^3\Delta_3$ and [19.0]2–$X^3\Delta_2$ transitions

It is well-known that information from isotopic molecules can be used to confirm the carrier of the spectrum. In this work, we recorded the (0, 0) band of the [18.6]3–$X^3\Delta_3$ and [19.0]2–$X^3\Delta_2$ transitions of both $Co^{10}B$ and $Co^{11}B$ isotopes. Molecular parameters of isotopic molecules are approximately related by different powers of the mass dependence $\rho = (\mu/\mu_i)$, where μ and μ_i are the reduced masses of $Co^{11}B$ and one of the isotopes, respectively. Since $Co^{11}B$ is the most abundant isotope, isotopic effects are calculated relative to it. The line list of the $\Delta\Omega = 0$ transitions with $\Omega'' = 2$ and $\Omega'' = 3$ is available from the supplemental material.[13] Table I also presents the observed molecular constants for both isotopic molecules; the values in parentheses are molecular constants calculated for the $Co^{10}B$ isotope from those of $Co^{11}B$ using the isotopic relationship.[12] The agreement of these molecular constants is very good, which confirms the carrier of the spectrum is CoB undoubtedly. The sizeable difference between the band origins of the $Co^{10}B$ and $Co^{11}B$ isotopes reflects a large isotope effect of the vibrational constants for the electronic states. Since we measured only one vibrational band of these two electronic transitions and it is difficult to confirm the relative intensity of the branches; we just identify these bands using their Ω values, namely, the [19.0]2–$X^3\Delta_2$ and the [18.6]3–$X^3\Delta_3$ transitions. Figure 4 summarizes all transition bands observed in this work.

E. Electronic configuration and the electronic states

In order to better understand the electronic structure of CoB, we would like to examine molecules formed from Co and the 2*p* main group elements such as CoC to CoO. Using the molecular orbital (MO) energy level diagram discussed by Merer and co-workers[14,15] for CoC and CoO, the MO energy levels formed are with 4*s* and 3*d* atomic orbitals (AOs) of the Co atom and the 2*p* AO of a main group element. Figure 5

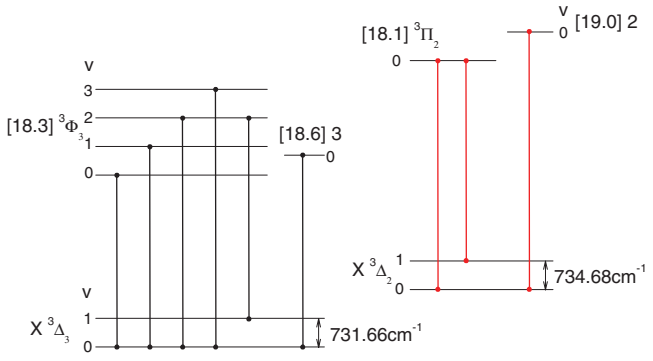

FIG. 4. Observed vibrational transitions of CoB.

represents qualitatively the relative energy order of the MOs formed from the Co and B atoms. The lower energy 8σ and 3π MOs and the higher energy 10σ and 4π MOs are formed from the main group $2p$ AO and Co $3d\sigma$, $3d\pi$ and $4p\sigma$ and $4p\pi$ AOs. The 9σ MO is essentially the Co $4s$ AO. The 1δ MO is the Co $3d\delta$ AO, because there is no other δ symmetry orbital around. The ground state CoC (Ref. 15) and CoN (Ref. 16) are

$$\mathrm{CoC}(X^2\Sigma^+): \quad (8\sigma)^2(3\pi)^4(1\delta)^4(9\sigma)^1 \quad \rightarrow \quad {}^2\Sigma^+, \qquad (2)$$

$$\mathrm{CoN}(X^1\Sigma^+): \quad (8\sigma)^2(3\pi)^4(1\delta)^4(9\sigma)^2 \quad \rightarrow \quad {}^1\Sigma^+. \qquad (3)$$

The Aufbau principle works very well in atoms, it is also possible to follow this thinking in adding electrons to the MOs in diatomic molecules. From Figure 5, we noticed that the energy of the 9σ and 1δ MOs are quite close; there could easily be two possible arrangements for the ground electron configuration for CoB so that adding one more electron could arrive at the configuration of CoC, they are either

$$(8\sigma)^2(3\pi)^4(1\delta)^4 \quad \rightarrow \quad {}^1\Sigma^+, \qquad (4)$$

$$\text{or} \quad (8\sigma)^2(3\pi)^4(1\delta)^3(9\sigma)^1 \quad \rightarrow \quad \mathrm{a}^1\Delta \text{ and } X^3\Delta_i. \qquad (5)$$

From the first lines of rotational branches, we concluded that the lower state has $\Omega = 3$ and $\Omega = 2$ spin components. Close examination of configurations of Eqs. (4) and (5) indicates

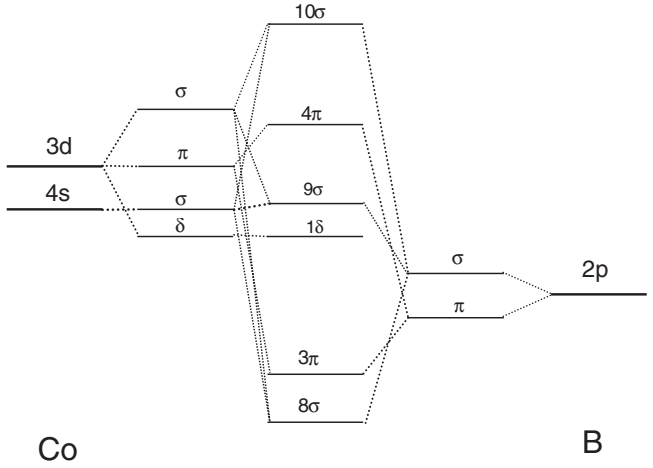

FIG. 5. Molecular orbital energy level diagram of CoB.

that only the $^3\Delta_i$ electronic state in Eq. (5) has $\Omega = 3$ and 2 components, therefore, the ground state of CoB is reasonable to be of the electronic configuration in Eq. (5). Since the number of electrons in the δ MO is more than half-filled, the $^3\Delta$ state arises from configuration of Eq. (5) is an inverted $^3\Delta$ state. For a $^3\Delta_i$ state, the $\Omega = 3$ component is the lowest in energy, and the $\Omega = 1$ component is of the highest energy. Our observation of the lower state with $\Omega = 2$ and 3 fits well with the $^3\Delta_i$ state to be the ground state. Another two pieces of information from our experimental work also indicate that the ground $^3\Delta$ state is an inverted state. First, the $\Omega = 2$ transitions are generally weaker in intensity than the $\Omega = 3$ transitions, which is consistent with the situation that the $\Omega = 2$ component is of lower population and is higher in energy than the $\Omega = 3$ component. Second, the effective B_{eff} value of an electronic state is given by the following expression:[12]

$$B_{eff} = B_v(1 + \Sigma B_v/\Lambda A), \qquad (6)$$

where B_v is the rotational constant for the v vibrational level and A is the spin-orbit constant for the electronic state, and Σ and Λ are quantum number of the projection of the spin and orbital angular momentum operators along the z-axis. Since the B_{eff} value of the $\Omega = 2$ (with $\Sigma = 0$) component is larger than the $\Omega = 3$ ($\Sigma = 1$) component, which implies that the spin-orbit constant, A, has a negative value. As far as the ground state electronic configuration of CoC is concerned, it has one more valence electron than CoB and that extra electron goes to the 1δ MO, which gives rise to the ground electronic configuration in Eq. (2).

Tzeli and Mavridis[8] performed multireference configuration interaction calculations on the *3d* transition metal monoborides employing a correlation consistent basis set of quintuple cardinality (5Z), and predicted the ground state to be $^3\Delta_i$ for CoB. Their calculated equilibrium bond length, $r_e = 1.700$ Å, is in good agreement with our determined value $r_o = 1.705$ Å for the $X^3\Delta_3$ state. Their calculated $\omega_e = 708\ \mathrm{cm}^{-1}$ compares reasonably well with our measured vibrational separation $\Delta G_{1/2} = 731.7\ \mathrm{cm}^{-1}$. In this work, we only observed parallel transitions and have no information on the spin-orbit components. It is possible to get some estimate of the magnitude of the spin-orbit parameter for the $X^3\Delta$ state from the atomic value of the cobalt atom, the 1δ orbital is essentially the Co $3d\delta$ AO, and Lefebvre-Brion and Field[17] tabulated a value of $\zeta = 530\ \mathrm{cm}^{-1}$ for Co atom. As a comparison, the spin-orbit constant, A, for the ground $X^4\Delta_i$ state of CoO (Ref. 18) with an electronic configuration of $(8\sigma)^2(3\pi)^4(1\delta)^3(4\pi)^2$ was determined to be $-332.4\ \mathrm{cm}^{-1}$. Since the first-order energy expression for calculating spin-orbit components is $A\Lambda\Sigma$, the separation between spin-orbit components is quite probable to be in hundreds of wavenumbers. Further work would be necessary to obtain the spin-orbit separations of the $X^3\Delta_i$ state.

In order to assign the upper state of our observed transitions, we assume single configuration can be used to describe the electronic states involved; we consider the promotion of an electron from either 1δ or 9σ MO in electronic configuration (5) to higher energy MO. If an electron was taken from the 1δ MO, the electronic configurations of the upper state

TABLE II. Comparison of molecular properties of the Group VIII A monoborides.

Molecule	CoB	RhB[a]	IrB[b]
Ground state	$^3\Delta_3$	$^1\Sigma^+$	$^3\Delta_3$
Electronic configuration[c]	$\delta^3\sigma^1$	δ^4	$\delta^3\sigma^1$
Bond length, r_o (Å)	1.705	1.614	1.767
$\Delta G_{1/2}$ (cm^{-1})	731.7	~920	909.6
Ground electronic. configuration of metal atom	$4s^2\ 3d^7$	$5s^1\ 6d^8$	$6s^2\ 5d^7$

[a]Reference 20.
[b]Reference 19.
[c]Electronic configuration giving rise to the ground state.

would be $\delta^2\sigma^1\sigma^1$ and also $\delta^2\sigma^1\pi^1$, in any case the spin multiplicities would be quintet, triplet, and singlet states, and the quintet states would be of lower energy. Since the ground state is basically a triplet state, for $\Delta S = 0$ transition, a triplet excited states is preferred. For promoting an electron from the 9σ to 4π MO, the following electronic configuration is obtained:

$$(8\sigma)^2(3\pi)^4(1\delta)^3\,(4\pi)^1 \quad \rightarrow \quad {}^1\Pi, {}^3\Pi_i, {}^1\Phi \text{ and } {}^3\Phi_i. \qquad (7)$$

The electronic configuration in Eq. (7) gives rise to four excited states of which the $^3\Pi_i$ and $^3\Phi_i$ have spin-orbit components with $\Omega = 2$ and $\Omega = 3$, respectively. For assigning the upper state, besides the $\Delta S = 0$ selection rule, we also based on the observed intensity pattern to establish $\Delta\Lambda$ values. The assignment of the $[18.1]^3\Pi_2$ state fits the $\Delta\Lambda = -1$ and $[18.3]^3\Phi_3$ state fits the $\Delta\Lambda = +1$ pattern. We, therefore, assigned the observed transitions as $[18.1]^3\Pi_2$–$X^3\Delta_2$ and $[18.3]^3\Phi_3$–$X^3\Delta_3$ systems. We are mindful that if the upper state is strongly mixed with nearby states, our assignment based on comparing relative intensity might not be valid. However, for the other two transition systems, we are not comfortable to make any assignment and only label them as [19.0]2 and [18.6]3 states.

It would be interesting to compare the spectroscopic properties of CoB with other monoborides in the same group. Table II lists the known spectroscopic properties of the group. The last line of the table also lists the ground electronic configuration of the transition metal atoms. It is easily seen from the table that the spectroscopic properties of CoB and IrB (Ref. 19) is quite similar including the ground state symmetry and electronic configuration, however, they are different from RhB.[20] These similarities between CoB and IrB can be ascribed to the atomic electronic configuration of the transition metals that gives rise to the ground state of the monoboride molecule, where the Co and Ir atoms have the s^2d^7 arrangement but the Rh atom has s^1d^8.

In summary, we report the first observation of electronic transition spectrum of CoB. Four transition systems have been observed and analyzed. The bond length, r_o, of the ground $X^3\Delta_3$ state has been determined to be 1.705 Å. The large hyperfine width observed in the spectral lines provides good support to having an unpaired electron in the 9σ ($4s\sigma$) orbital in the ground state.

ACKNOWLEDGMENTS

The work described here was supported by a grant from the Research Grants Council of the Hong Kong Special Administrative Region, China (Project No. HKU 701008).

[1]B. Ganem and J. O. Osby, Chem. Rev. **86**, 763 (1986).
[2]G. Will, J. Solid State Chem. **177**, 628 (2004).
[3]H. J. Choi, D. Roundy, H. Sun, M. L. Cohen, and S. G. Louie, Nature (London) **418**, 758 (2002).
[4]H. Chung, M. B. Weinberger, J. B. Levine, A. Kavner, J. Yang, S. H. Tolbert, and R. B. Kaner, Science **316**, 436 (2007).
[5]Y. Satio and M. Maida, J. Phys. Chem. A **103**, 1291 (1999).
[6]P. Krishnan, S. G. Advani, and A. K. Prasad, Appl. Catal., B **86**, 137 (2009).
[7]C. Yang, M. Chen, and Y. Chen, Int. J. Hydrogen Energy **36**, 1418 (2011).
[8]D. Tzeli and A. Mavridis, J. Chem. Phys. **128**, 034309 (2008).
[9]W. J. Balfour, P. K. Chowdhury, and R. Li, Chem. Phys. Lett. **463**, 25 (2008).
[10]Q. Ran, W. S. Tam, C. Ma, and A. S.-C. Cheung, J. Mol. Spectrosc. **198**, 175 (1999).
[11]H. F. Pang, Y. W. Ng, and A. S.-C. Cheung, Chem. Phys. Lett. **509**, 16 (2011).
[12]G. Herzberg, *Spectra of Diatomic Molecules* (Van Nostrand, New York, 1950).
[13]See supplementary material at http://dx.doi.org/10.1063/1.3663619 for the observed line positions of the [18.1] $^3\Pi_2$–$X^3\Delta_2$, [18.3] $^3\Phi_3$–$X^3\Delta_3$, [18.6]3–$X^3\Delta_3$, [19.0]2–$X^3\Delta_2$ transition.
[14]A. J. Merer, Annu. Rev. Phys. Chem. **40**, 407 (1989).
[15]B. Barnes, A. J. Merer, and G. F. Metha, J. Chem. Phys. **103**, 8360 (1995).
[16]L. Andrews, A. Citro, G. V. Chertihin, W. D. Bare, and M. Neurock, J. Phys. Chem. A **102**, 2561 (1998).
[17]H. Lefebvre-Brion and R. W. Field, *The Spectra and Dynamics of Diatomic Molecules* (Elsevier, New York, 2004).
[18]D. J. Clouthier, G. Huang, A. J. Merer, and E. J. Friedman-Hill, J. Chem. Phys. **99**, 6336 (1993).
[19]J. Ye, H. F. Pang, A. M.-Y. Wong, J. W.-H. Leung, and A. S.-C. Cheung, J. Chem. Phys. **128**, 154321 (2008).
[20]P. K. Chowdhury and W. J. Balfour, J. Chem. Phys. **124**, 216101 (2006).